Polymer Journal (2019) 51:685–692
https://doi.org/10.1038/s41428-019-0177-4

ORIGINAL ARTICLE

Sonoporation-based labeling of mesenchymal stem cells with polymeric MRI contrast agents for live-cell tracking

Atsushi Mahara[1] · Naoki Kobayashi[1,2] · Yoshiaki Hirano[2] · Tetsuji Yamaoka[1]

Received: 27 December 2018 / Revised: 23 January 2019 / Accepted: 28 January 2019 / Published online: 28 February 2019

Abstract

Cell transplantation has the potential to improve repair of injured tissue function; however, it is not clear how transplanted cells participate in functional recovery. We have recently succeeded in tracking millions of transplanted living cells using a polymeric MRI contrast agent, which was delivered into monolayer-cultured cells through electroporation. However, when cells were labeled using a conventional electroporation method, only cells localized around the electrode were labeled. To improve the percentage of labeled cells and to be able to start with fewer cells, we focused on a homogeneous cell labeling system. In this study, we optimized the sonoporation of a suspension culture with microbubbles for labeling and MR tracking of mesenchymal stem cells (MSCs). When water was used as the transmission medium between the acoustic probe and cell suspension, microbubbles gently collapsed with minimal cell damage. Under this condition, the number of labeled MSCs was 25%, which is 3.3-fold greater than the number of MSCs labeled using the previous system, and the cell viability was maintained at approximately 80%. The MRI signal could be clearly observed for 2.0×10^6 MSCs. These results suggest that sonoporation can efficiently introduce the polymeric contrast agent into MSCs.

Introduction

Recently, stem cell therapy has made significant contributions to the treatment of patients with Parkinson's disease [1, 2], limb ischemia [3], multiple sclerosis [4], tumors [5], and ischemic heart failure [6–9]. Although functional recovery by the engrafted cells [10] and immunosuppressive production have been proposed [11] as the mechanisms of action, the viability of the transplanted cells has not been fully elucidated [4, 7, 12].

Superparamagnetic iron oxide (SPIO) has been widely studied as a labeling agent to track transplanted cells on a magnetic resonance imaging (MRI) scan. It is released from cells upon cell death and remains in the surrounding tissues, where it is possibly taken up by macrophages [13]. In our previous work, water-soluble polymeric MRI contrast agents were developed for in vivo living-cell tracking [14–17]. Poly(vinyl-alcohol) and dextran were selected for constructing the main chain of the contrast agent, and gadolinium (Gd)-chelate was conjugated to these polymers. Once introduced into cells, such contrast agents exist stably within the cells without inhibiting cell growth or differentiation and do not leak out while the cells are alive [14]. Upon cell death, the contrast agents leak into the bloodstream and are excreted into urine without any nonspecific accumulation in the tissue. Therefore, only living labeled cells can be visualized through MRI. Using these contrast agents, we also observed the migration of endothelial progenitor cells from transplantation sites to ischemic areas [15].

To introduce the contrast agents into cells, electroporation was carried out on monolayer-cultured cells, and we have previously succeeded in visualizing 5×10^6 cells on an MRI scan [17]. Electroporation has already been established as a technique for use in medicine and biotechnology [18, 19]. The electric field generates pores in the cell membrane [18], and substrates can then permeate into cells through the

Supplementary information The online version of this article (https://doi.org/10.1038/s41428-019-0177-4) contains supplementary material, which is available to authorized users.

✉ Tetsuji Yamaoka
yamtet@ncvc.go.jp

[1] Department of Biomedical Engineering, National Cerebral and Cardiovascular Center Research Institute, Fujishiro-dai, Suita, Osaka 565-8565, Japan

[2] Faculty of Chemistry, Materials and Bioengineering, Kansai University, 3-3-35 Yamatecho, Suita, Osaka 565-8680, Japan

pores. The efficiency depends on the strength of the electric field. Moreover, it has also been reported that permeability depends on the electrical charge of the substrate [20].

In the present study, the sonoporation of a suspension of cells with microbubbles was investigated to increase the number of labeled cells. The introduction of substrates into the cell by sonoporation is generally attributed to permeation through the transient pore of the cell membrane produced by acoustic cavitation of the microbubbles [21]. Through the sonoporation of the suspension, acoustic cavitation from homogeneously dispersed microbubbles evenly generates pores in the cell membrane, resulting in an increase in the number of labeled cells containing contrast agent. On the other hand, since excess cavitation can be cytotoxic, the microbubble concentration and the acoustic intensity should be optimized to achieve both high cell viability and a high percentage of labeled cells. Here, the number and viability cells labeled by sonoporation in suspension were quantitatively analyzed. The MR signals of mesenchymal stem cells (MSCs) labeled by sonoporation and conventional electroporation were also compared. The optimized sonoporation condition showed a 3.3-fold greater number of labeled cells compared with that of conventional sonoporation in a monolayer system, and a 2.0×10^6 MSC suspension could be visualized on an MRI scan.

Materials and methods

Synthesis of Gd-Dextran

Gd-chelate-conjugated dextran (Gd-Dextran, Fig. 1a) was synthesized according to our previous reports (Supporting Fig. 1) [16]. In brief, dextran (10×10^{-3} unit mol, 20 kDa; Wako Pure Chemical Industries Inc., Japan) was combined with 1,3-propane diamine (PD) by means of a coupling agent, 1,1′-carbonylbis-[1H-imidazole] (CDI). The feeder ratio of CDI and PD to the glucopyranose unit of dextran was 5:1 and 50:1, respectively. Dextran containing an amino group in 25% of its glucopyranose units was used in the following reaction. The introduction rate of PD to dextran was determined by using a 300 MHz NMR spectrometer (Gemini2000/300; Varian Inc., CA, USA). In the next step, aminated dextran was labeled with fluorescein isothiocyanate (FITC, Sigma-Aldrich, NY) and then subsequently combined with mono-N-succinimidyl 1,4,7,10-tetraazacyclododencane-1,4,7,10-tetraacetate (DOTA; Nard Institute, Ltd, Hyogo, Japan) as a chelator of Gd. The feeder ratio of FITC and DOTA to the amino groups of aminated dextran was 1:250 and 3:1, respectively. The introduction of FITC was confirmed by UV spectroscopy (UV-1650PC, Shimadzu, Japan). The introduction ratio of DOTA to dextran was determined using a 300 MHz NMR spectrometer, and it was found that 17% of the glucopyranose units of the dextran were modified with the DOTA (Supporting Fig. 2). Eight percent of the glucopyranose units of the dextran were free amino groups. Finally, DOTA and fluorescein-conjugated dextran were chelated with Gd. In this reaction, the feeder ratio of $GdCl_3 \cdot 6H_2O$ to DOTA of the dextran was 3:1. After the reaction at each step, the samples were purified with a dialysis membrane (MWCO of 3500; Spectrum Laboratories Inc., Houston TX). Using inductively coupled plasma atomic emission spectroscopy (Model 7510; Shimadzu Co., Kyoto, Japan), we confirmed that the DOTA in the dextran was completely chelated with the Gd. The obtained dextran is referred to as Gd-dextran in the following section.

MSCs and cell viability assay

All animal experiments were conducted in accordance with the Guidelines for Animal Experiments established by the Ministry of Health, Labor, and Welfare of Japan and by the National Cerebral and Cardiovascular Center Research Institute in Japan. The protocol was approved by the Committee on the Ethics of Animal Experiments of the National Cerebral and Cardiovascular Center Research Institute (Permit Number: 009017). MSCs were isolated from bone marrow (BM) flushed from the femurs of Sprague Dawley (SD) rats (SLC Japan Inc., Shizuoka, Japan). The BM was seeded on collagen-coated dishes and was cultured in alpha-MEM (α-MEM, Gibco, NY) supplemented with 15% fetal bovine serum for 48 h. The adherent cell populations were cultured as MSCs until experimental use.

The WST-1 viability assay was carried out according to the manufacture's protocol (Takara Shuzo, Otsu, Japan). Briefly, cells were washed with phosphate-buffered saline (PBS), and culture medium (100 µl) was added to each well. Ten microliters of WST-1 solution were added to each well, and the cells were incubated for 30 min. Absorbance was measured at 450 nm using a microplate reader (Model 550; Bio-Rad Laboratory Co., Tokyo, Japan).

Electroporation and sonoporation

To save cost and time, commercially available fluorescein-conjugated dextran (F-Dextran, 15 kDa; Sigma-Aldrich, NY) was used as the model molecule of the polymeric contrast agents for optimizing electroporation and sonoporation conditions. In the case of electroporation, MSCs were cultured in a 6 cm diameter dish at a concentration of 5×10^5 cells per dish for 1 day prior to electroporation. F-dextran was added to the culture medium at a concentration of 10 mM, and electrical pulses were applied to the cells using an electroporator (CUY-21; NepaGene Co., Ltd,

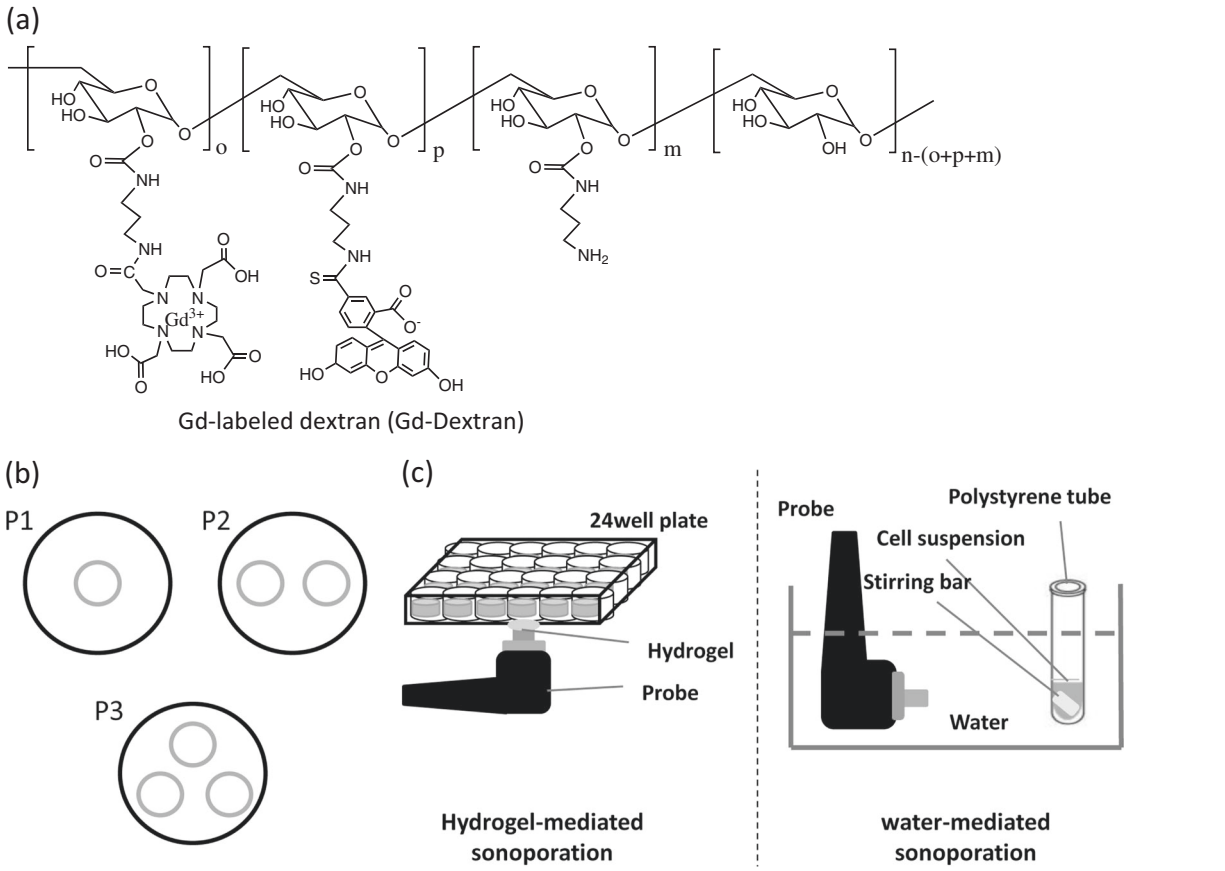

Fig. 1 Polymeric contrast agent and cell labeling procedure. **a** Chemical structure of gadolinium (Gd)-labeled dextran. The shown structure is one representative form of varying derivatives. **b** Three different positions for electroporation were examined. Electric pulses were applied to 1, 2, or 3 positions in the 6 cm culture dish indicated by blue circles as P1, P2, and P3, respectively. **c** Hydrogel and water were used as the transmission media for sonoporation. In hydrogel-mediated sonoporation, the probe contacted the 24-well plate via the hydrogel (**c**, left). In water-mediated sonoporation, the probe was set 8 cm away from the sample tube (**c**, right). The water temperature was set to 37 °C

Tokyo, Japan). Rectangular electrical pulses (field strength 300 V/cm, number of pulses 10, pulse duration 5 ms) were applied to the cells using two parallel electrodes with a 5 mm gap. The electrical pulses were applied at one, two, or three places on the culture dish, which were abbreviated as P1, P2, and P3, respectively. The applying positions are illustrated in Fig. 1b.

In the case of sonoporation, MSCs in the suspension (1×10^6 cells/ml) were mixed with microbubbles (Sonazoid^{TM}; Daiichi-Sankyo, Tokyo, Japan). The ratio of microbubbles to cells was controlled at 25:1, 50:1, or 100:1. The F-dextran was mixed at a concentration of 10 mM. Acoustic power was applied by using a commercially available generator (Sonitron 2000; NepaGene Co., Ltd, Tokyo, Japan).

Water and hydrogel (Signa Gel, Parker Laboratories, Inc., NJ) were used as transmission media between the acoustic probe and the specimens (Fig. 1c). The ultrasound frequency was fixed as 1 MHz. The acoustic powers in the case of hydrogel- and water-mediated sonoporation were tuned as 0.1–2.0 and 1.0–4.0 W/cm^2, respectively. Exposure times (duty cycle; 20%) of the acoustic power in the cases of hydrogel- and water-mediated sonoporation were 10 and 120 s, respectively. When hydrogel-mediated sonoporation was performed, the MSC suspension was placed in a 24-well plate (Iwaki Glass, Tokyo, Japan). Contact was made between the acoustic probe and the bottom of the well via the hydrogel, and ultrasound was applied. After ultrasound irradiation, the MSCs were collected and washed with PBS. When water-mediated sonoporation was performed, the MSC suspension was placed in a 5 ml polystyrene round-bottom tube (BD Falcon, Bedford, MA). The acoustic probe and sample tube were placed in a water bath (37 °C) at a distance of 8 cm. After irradiation, the MSC suspension was washed with PBS. To measure the number of remaining microbubbles before and after the acoustic irradiation, the microbubble numbers were counted using a hemocytometer.

For MRI experiments, the electric pulse was applied at position three (P3) when the MSCs were labeled with

Gd-dextran by electroporation. When the MSCs were labeled by sonoporation, water-mediated sonoporation was conducted with 4 W/cm^2 of acoustic power and a 1:100 ratio of microbubbles to cells. After cell labeling by electroporation and sonoporation, the cells were washed with PBS, and then MR images were acquired.

Flow cytometry

The number of MSCs labeled with F-dextran and Gd-dextran were counted using a fluorescent activated cell sorter (FACS; FACSCalibur; BD Bioscience, San Jose, CA). The analysis was carried out following the standard procedure. To calculate the labeling ratio of MSCs based on FACS data, the peak shifted from the histograms of non-labeled MSCs was considered as the signals from labeled MSCs. The fluorescence intensity at the valley between the peaks derived from nonlabeled and labeled MSCs was set as the threshold, and the labeling ratio was calculated.

MRI measurements

The MRI was acquired using the T1-weighted image protocol on a 1.5-T compact MRI system (MRmini; Dainippon Sumitomo Pharma, Osaka, Japan). The repetition time (TR) and echo time (TE) were set to 300 and 9 ms, respectively (field of view [FOV], 4 × 8 cm; matrix, 126 × 256; slice thickness, 1 mm; slice gap, 0 mm; number of slices, 35).

Results and discussion

Labeling of MSCs by electroporation

The labeling efficiency and viability of MSCs were evaluated using a fluorescence microscope 24 h after electroporation. Cells on the electrodes were detached from the culture dish (Fig. 2a). The viability tended to decrease when the electrical pulse was applied in multiple places and reached approximately 70% after electroporation at P3 (Fig. 2b). Labeled MSCs were observed only near the electrodes, and MSCs localized far from the electrode were not labeled, resulting in a lower percentage of labeled MSCs.

Electroporation is a conventional method for transporting substances into cells without any specific interaction with the cell membrane. Micropores in the cell membrane are temporarily formed by the electric pulse, and then, the substrate, such as polymers or DNA, enters directly through the micropore [22]. It has been reported that proteins and polysaccharides are effectively introduced into the cell by electroporation [23]. Glogauer et al. [24] reported that proteins of up to 66 kDa could be incorporated into fibroblast cells with approximately 80% viability under optimized conditions. It has also been reported that serum albumins and dextrans with molecular weights of 500 kDa were introduced into 80–90% of dictyostelium [25]. On the other hand, it was also observed that the electroporation threshold depended on the species of the cells [26]. In our previous study, 5×10^6 MSCs labeled by conventional electroporation were detected on MRI [17]. To track lower numbers of cells, it will be necessary to label a large proportion of the cells with a polymeric contrast agent. When MSCs were labeled through electroporation in a monolayer system, only MSCs localized near the electrodes were labeled, and the number of labeled MSCs was limited. To increase the number of labeled MSCs, we optimized the labeling conditions by using sonoporation in a suspension system.

Labeling of MSCs by sonoporation

The remaining number of microbubbles was plotted against the irradiation time and acoustic power (Fig. 3). When hydrogel was used as the transmission medium (Fig. 1c), the number of microbubbles rapidly decreased at an irradiation power of 0.2 and 1.5 W/cm^2. The microbubbles had completely disappeared after 10 s. When water was used as the transmission medium, the number of microbubbles gradually decreased even if the irradiation intensity was set as 2.0 W/cm^2 (Fig. 3). Under this condition, the microbubbles disappeared in 60 s. The microbubbles disappeared more quickly when hydrogel was used as the transmission medium. From these results, irradiation times under hydrogel- and water-mediated conditions were set to 10 and 120 s, respectively.

The acoustic power and influence of the microbubble concentration on the number of labeled MSCs and viability were investigated (Fig. 4). When hydrogel was used as the transmission medium, the number of labeled MSCs increased with the acoustic power (Fig. 4a). The number of labeled cells reached 40% when the power was set as 2.0 W/cm^2. A similar tendency was also observed when water was used as the medium (Fig. 4c). However, the number of labeled cells was smaller than that under the hydrogel-mediated condition, and the proportion was only approximately 25%.

The viability of MSCs decreased sharply to approximately 20% after irradiation under hydrogel-mediation conditions (Fig. 4b). When water was used as the transmission medium, the viability was maintained at approximately 80% (Fig. 4d). The ratio of microbubbles to MSCs did not affect the number of labeled MSCs or viability. These results clearly indicated that MSCs could be labeled by water-mediated sonoporation with minimal cell damage. The number of MSCs labeled using sonoporation was

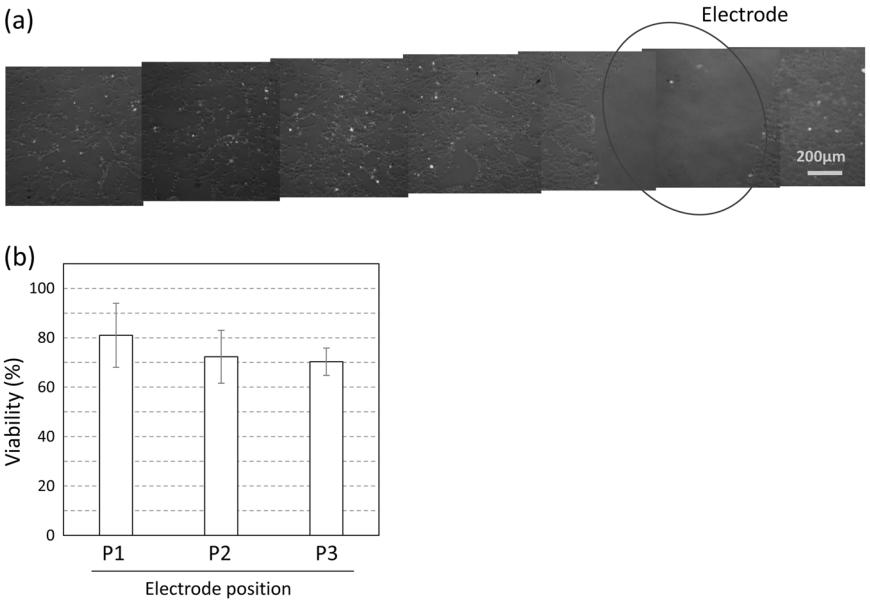

Fig. 2 Labeling of MSCs by electroporation. **a** Fluorescent images around the electrode position after electroporation. **b** Cell viability after the electroporation was quantified using the WST-1 assay. The value is indicated as the mean ± S.D. ($n = 3$)

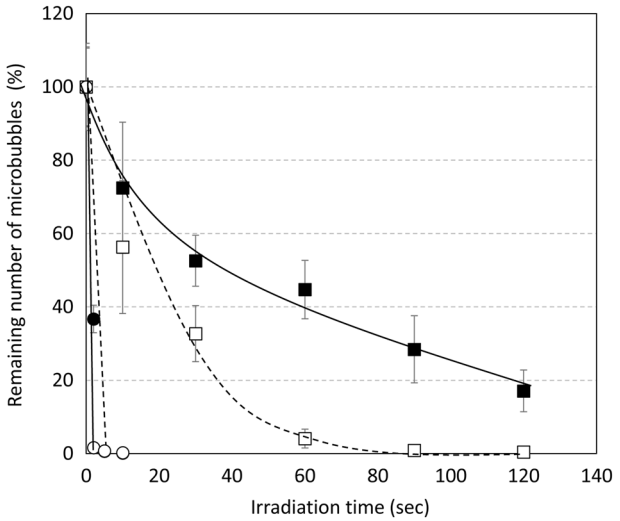

Fig. 3 Effect of irradiation time and acoustic powers on the remaining number of microbubbles was plotted. In the hydrogel-mediated sonoporation, acoustic power was tuned to 0.2 (filled circle) and 1.5 (open circle) W/cm^2. In the case of water-mediated sonoporation, the power was tuned as 1.5 (filled square) and 2.0 (open square) W/cm^2. The value is indicated as the mean ± S.D. ($n = 3$)

3.3-fold larger compared with the labeling ratio of 7.5% in a conventional electroporation condition.

It has been reported that polymers of 10 to 2000 kDa molecular weight could be introduced into cells by sonoporation [27, 28]. It has previously been suggested that loading mechanisms include diffusion not only through cell membrane pores but also via endocytosis [28, 29]. In our study, the contrast agents were not incorporated into the cells without acoustic power irradiation. Although the possibility of endocytosis could not be completely excluded by our experimental data alone, the mechanism in our study appears to be mainly dependent on diffusion during sonoporation. In general, the cell viability and labeling efficiency are affected by microbubble concentration and acoustic powers [30]. In our experiments, the viability of MSCs decreased with increasing acoustic power when hydrogel was used as the transmission medium. The acoustic energy largely attenuates with not only distance but also the transmission media between the probe and specimen. In the case of hydrogel-mediated sonoporation, the acoustic power is effectively transmitted compared with water-mediated conditions. Under hydrogel-mediated sonoporation, the rapid collapse of microbubbles occurred in a short time (Fig. 3), and serious damage could be induced in the cells. In contrast, the microbubbles gradually decomposed under water-mediated sonoporation, and the cell viability could be maintained by avoiding serious destruction of the cell membrane. Unfortunately, more detailed speculation related to the labeling mechanisms cannot be discussed with the limited data available, and further investigation is necessary.

Imaging of labeled MSCs on MRI

To evaluate signal enhancing on MRI, MSCs were labeled with Gd-dextran using the optimized sonoporation condition. The number of labeled MSCs was counted by FACS (Fig. 5a). After labeling by sonoporation, two peaks were observed on the FACS analysis, and 52.2% of the cells were labeled with Gd-dextran (Fig. 5a). This higher value than the result shown in Fig. 4c is derived from electric property of the F-dextran and Gd-dextran. The Gd-dextran contains 8% of free amino groups, and its surface charge would be slightly positive compared with that of F-dextran.

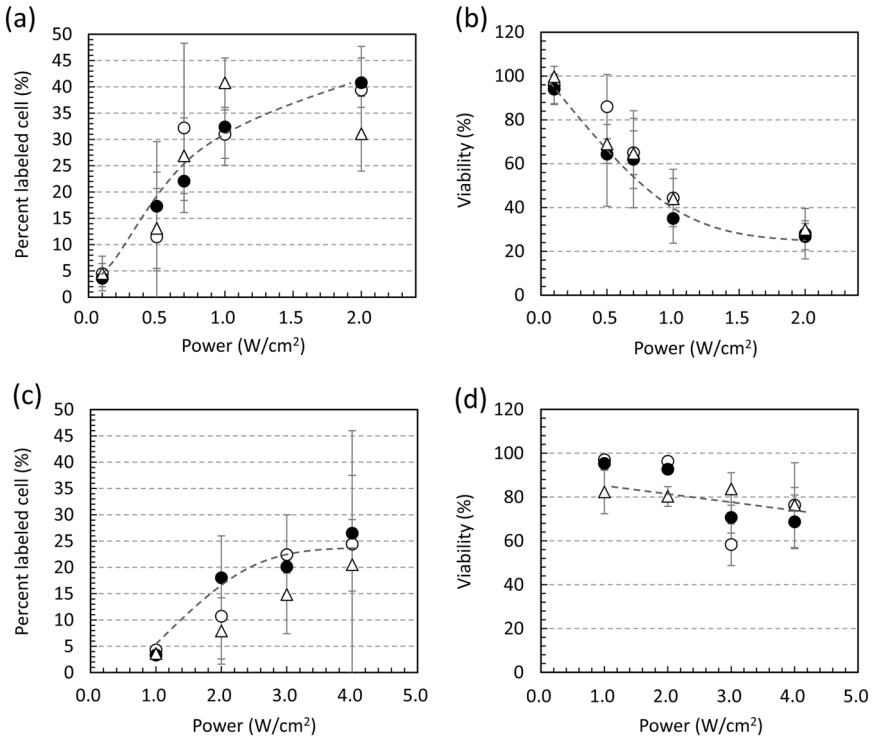

Fig. 4 Percentage of labeled cells and viability of MSCs plotted as the function of acoustic power. The cells were treated with **a**, **b** hydrogel-mediated sonoporation or **c**, **d** water-mediated sonoporation. The ratio of microbubbles to cells was controlled as 25:1 (open circle), 50:1 (filled circle), or 100:1 (open triangle). Cell viability and percentage of labeled cells were quantified by WST-1 assay and FACS analysis, respectively. The value is indicated as the mean ± S.D. ($n = 3$)

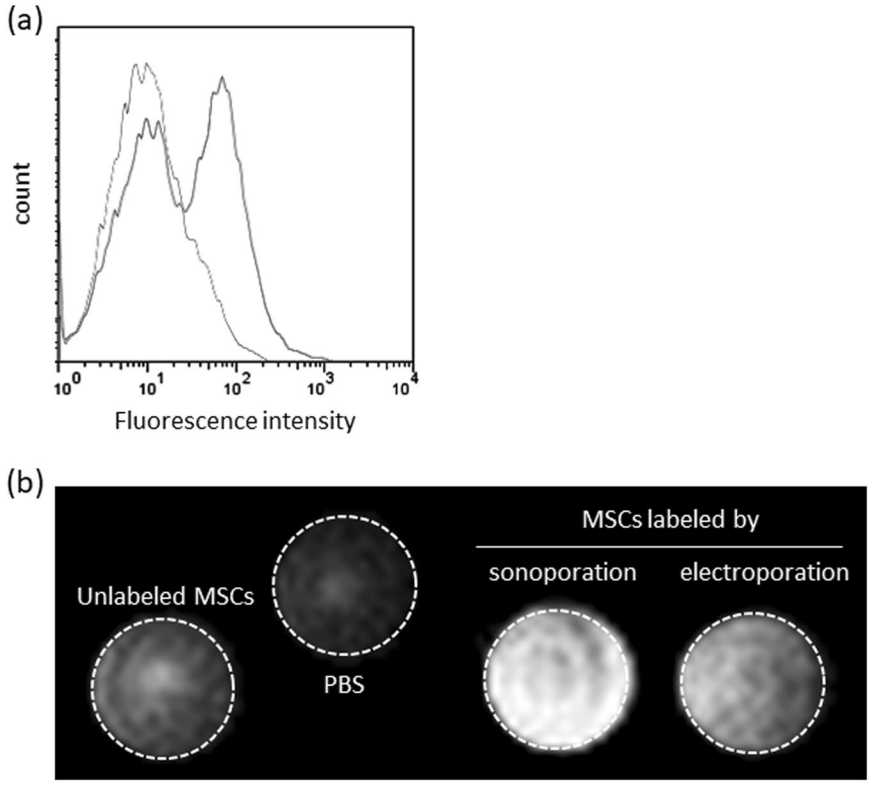

Fig. 5 MR imaging of MSCs labeled with Gd-dextran by electroporation or sonoporation. **a** The number of MSCs labeled by sonoporation was counted by FACS. The black line indicates unlabeled MSCs and the blue line indicates labeled MSCs. **b** MR images of PBS, unlabeled MSCs, and MSCs labeled by sonoporation or electroporation are indicated. The cell number was 2×10^6

Therefore, the Gd-dextran could easily access cell membranes, and the labeling rate would increase. The internalization efficiency of Gd-dextran per single cell is also important when discussing cell labeling efficiency. Based on the FACS analysis, the mean fluorescence intensity of MSCs labeled with Gd-dextran using sonoporation was similar to that using electroporation. Therefore, we considered that internalization efficiency of Gd-dextran was the same between them.

The T1-weighted MR images of the labeled MSCs are shown in Fig. 5b. The MR signals of PBS and unlabeled MSCs were almost same as that of MSCs labeled by electroporation. The signal of the MSCs labeled by sonoporation was clearly enhanced compared with that under other conditions. These data indicated that 2×10^6 of MSCs could be clearly identified on MRI. To investigate the therapeutic effect of transplanted cells, greater than approximately 10^6 MSCs are generally transplanted into rat models [31, 32]. Under our previous condition, 5 to 10×10^6 cells were required for tracking cells on MIR [17]. In this study, the number of MSCs required for detection on MRI could be reduced by optimizing the sonoporation condition. We showed here the possibility that MSCs can be traced with high sensitivity using a polymeric contrast agent.

In this study, we succeeded in optimizing the labeling condition of MSCs while minimizing cell death by using a water-mediated sonoporation method. The detectable number of MSCs on MIR could be reduced by optimizing the sonoporation condition, and we could visualize almost the same number of MSCs as routinely used in cell transplantation studies. Our findings in this study will be helpful for in vivo cell tracking by MRI in cell transplantation studies.

Acknowledgements The authors acknowledge financial support from the JSPS KAKENHI (Grant Number JP15K01308) and the Intramural Research Fund of National Cerebral and Cardiovascular Center (25-2-2).

Compliance with ethical standards

Conflict of interest The authors declare that they have no conflict of interest.

References

1. Kefalopoulou Z, Politis M, Piccini P, Mencacci N, Bhatia K, Jahanshahi M, et al. Long-term clinical outcome of fetal cell transplantation for Parkinson disease: two case reports. JAMA Neurol. 2014;71:83–7.
2. Hurtado JDC, Sánchez JPB, Nunes RB, de Oliveira AA. Stem cell transplantation and physical exercise in Parkinson's disease, a literature review of human and animal studies. Stem Cell Rev. 2017. https://doi.org/10.1007/s12015-017-9798-1.
3. Tateishi-Yuyama E, Matsubara H, Murohara T, Ikeda U, Shintani S, Masaki H, et al. Therapeutic angiogenesis for patients with limb ischaemia by autologous transplantation of bone-marrow cells: a pilot study and a randomised controlled trial. Lancet. 2002;360:427–35.
4. Frau J, Carai M, Coghe G, Fenu G, Lorefice L, La Nasa G, et al. Long-term follow-up more than 10 years after HSCT: a monocentric experience. J Neurol. 2018;265:410–6.
5. Armand P, Nagler A, Weller EA, Devine SM, Avigan DE, Chen YB, et al. Disabling immune tolerance by programmed death-1 blockade with pidilizumab after autologous hematopoietic stem-cell transplantation for diffuse large B-cell lymphoma: results of an international phase II trial. J Clin Oncol. 2013;31:4199–206.
6. Perin EC, Dohmann HF, Borojevic R, Silva SA, Sousa AL, Mesquita CT, et al. Transendocardial, autologous bone marrow cell transplantation for severe, chronic ischemic heart failure. Circulation. 2003;107:2294–302.
7. Meyer GP, Wollert KC, Lotz J, Pirr J, Rager U, Lippolt P, et al. Intracoronary bone marrow cell transfer after myocardial infarction: 5-year follow-up from the randomized-controlled BOOST trial. Eur Heart J. 2009;30:2978–84.
8. Menasché P, Alfieri O, Janssens S, McKenna W, Reichenspurner H, Trinquart L, et al. The Myoblast Autologous Grafting in Ischemic Cardiomyopathy (MAGIC) trial: first randomized placebo-controlled study of myoblast transplantation. Circulation. 2008;117:1189–200.
9. Sawa Y, Miyagawa S, Sakaguchi T, Fujita T, Matsuyama A, Saito A, et al. Tissue engineered myoblast sheets improved cardiac function sufficiently to discontinue LVAS in a patient with DCM: report of a case. Surg Today. 2012;42:181–4.
10. Kim SW, Han H, Chae GT, Lee SH, Bo S, Yoon JH, et al. Successful stem cell therapy using umbilical cord blood-derived multipotent stem cells for Buerger's disease and ischemic limb disease animal model. Stem Cells. 2006;24:1620–6.
11. Djouad F, Plence P, Bony C, Tropel P, Apparailly F, Sany J, et al. Immunosuppressive effect of mesenchymal stem cells favors tumor growth in allogeneic animals. Blood. 2003; 102:3837–44.
12. Lunde K, Solheim S, Aakhus S, Arnesen H, Abdelnoor M, Egeland T, et al. Intracoronary injection of mononuclear bone marrow cells in acute myocardial infarction. N Engl J Med. 2006;355:1199–209.
13. Amsalem Y, Mardor Y, Feinberg MS, Landa N, Miller L, Daniels D, et al. Iron-oxide labeling and outcome of transplanted mesenchymal stem cells in the infarcted myocardium. Circulation. 2007;116:I38–45.
14. Tachibana Y, Enmi J, Mahara A, Iida H, Yamaoka T. Design and characterization of a polymeric MRI contrast agent based on PVA for in vivo living-cell tracking. Contrast Media Mol Imaging. 2010;5:309–17.
15. Agudelo CA, Tachibana Y, Hurtado AF, Ose T, Iida H, Yamaoka T. The use of magnetic resonance cell tracking to monitor endothelial progenitor cells in a rat hindlimb ischemic model. Biomaterials. 2012;33:2439–48.
16. Agudelo CA, Tachibana Y, Yamaoka T. Synthesis, properties, and endothelial progenitor cells labeling stability of dextrans as polymeric magnetic resonance imaging contrast agents. J Biomater Appl. 2013;28:473–80.
17. Tachibana Y, Enmi J, Agudelo CA, Iida H, Yamaoka T. Long-term/bioinert labeling of rat mesenchymal stem cells with PVA-Gd conjugates and MRI monitoring of the labeled cell survival after intramuscular transplantation. Bioconjug Chem. 2014;25:1243–51.
18. Weaver JC, Chizmadzhev YA. Theory of electroporation: a review. Bioelectrochem Bioenerg. 1996;41:135–60.

19. Yarmush ML, Golberg A, Serša G, Kotnik T, Miklavčič D. Electroporation-based technologies for medicine: principles, applications, and challenges. Annu Rev Biomed Eng. 2014;16:295–320.
20. Paganin-Gioanni A, Bellard E, Escoffre JM, Rols MP, Teissié J, Golzio M. Direct visualization at the single-cell level of siRNA electrotransfer into cancer cells. Proc Natl Acad Sci USA. 2011;108:10443–7.
21. Lentacker I, De Cock I, Deckers R, De Smedt SC, Moonen CT. Understanding ultrasound induced sonoporation: definitions and underlying mechanisms. Adv Drug Deliv Rev. 2014;72:49–64.
22. Kotnik T, Frey W, Sack M, Haberl Meglič S, Peterka M, Miklavčič D. Electroporation-based applications in biotechnology. Trends Biotechnol. 2015;33:480–8.
23. Bright GR, Kuo NT, Chow D, Burden S, Dowe C, Przybylski RJ. Delivery of macromolecules into adherent cells via electroporation for use in fluorescence spectroscopic imaging and metabolic studies. Cytometry. 1996;24:226–33.
24. Glogauer M, McCulloch CA. Introduction of large molecules into viable fibroblasts by electroporation: optimization of loading and identification of labeled cellular compartments. Exp Cell Res. 1992;200:227–34.
25. Yumura S, Matsuzaki R, Kitanishi-Yumura T. Introduction of macromolecules into living Dictyostelium cells by electroporation. Cell Struct Funct. 1995;20:185–90.
26. Tarek M. Membrane electroporation: a molecular dynamics simulation. Biophys J. 2005;88:4045–53.
27. Karshafian R, Samac S, Bevan PD, Burns PN. Microbubble mediated sonoporation of cells in suspension: clonogenic viability and influence of molecular size on uptake. Ultrasonics. 2010;50:691–7.
28. Delalande A, Kotopoulis S, Postema M, Midoux P, Pichon C. Sonoporation: mechanistic insights and ongoing challenges for gene transfer. Gene. 2013;525:191–9.
29. Meijering BD, Juffermans LJ, van Wamel A, Henning RH, Zuhorn IS, Emmer M, et al. Ultrasound and microbubble-targeted delivery of macromolecules is regulated by induction of endocytosis and pore formation. Circ Res. 2009;104:679–87.
30. Wang M, Zhang Y, Cai C, Tu J, Guo X, Zhang D. Sonoporation-induced cell membrane permeabilization and cytoskeleton disassembly at varied acoustic and microbubble-cell parameters. Sci Rep. 2018;8:3885.
31. Guarita-Souza LC, Carvalho KA, Rebelatto C, Senegaglia A, Hansen P, Furuta M, et al. Cell transplantation: differential effects of myoblasts and mesenchymal stem cells. Int J Cardiol. 2006;111:423–9.
32. Kinnaird T, Stabile E, Burnett MS, Shou M, Lee CW, Barr S, et al. Local delivery of marrow-derived stromal cells augments collateral perfusion through paracrine mechanisms. Circulation. 2004;109:1543–9.